ELSEVIER

Thin Solid Films 335 (1998) 146–152

thin solid films

Formation of Cr—O and Cr—N—O films serving as Cu oxidation resistant layers and their N_2 pre-sintering effect

Jui-Chang Chuang*, Mao-Chieh Chen

Department of Electronics Engineering and the Institute of Electronics, National Chiao-Tung University,1001 Ta Hsueh Road, Hsinchu, 300, Taiwan

Received 19 March 1998; accepted 12 June 1998

Abstract

This study investigates the Cu oxidation resistant layers of sputter deposited Cr—O and reactively sputter deposited Cr—N—O of 200 Å thickness, with and without, thermal N_2 pre-sintering treatment. The resistance against Cu oxidation (or the highest annealing temperatures without causing Cu oxidation) of the Cr—O and Cr—N—O covered Cu films were found to be 350 and 500°C, respectively, in an O_2 ambient. The inherent defects in the Cr—O layers and the nitrogen doping in the Cr—N—O layers were believed to be the principal causes for the distinction of the resistance against Cu oxidation. With N_2 pre-sintering treatments on the Cr—O or Cr—N—O covered Cu films, the ability of resistance against Cu oxidation was degraded. The higher the N_2 pre-sintering temperature was, the lower the oxidation temperature of Cu became. The N_2 pre-sintering thermal process led to formation of defects on the Cr—O and Cr—N—O layers, resulting in the degradation of the ability of resistance against Cu oxidation. Thus, the application of Cr—O or Cr—N—O as a resistant layer against Cu oxidation should avoid such an excess thermal treatment.

Keywords: Chromium; Copper; Oxidation; X-ray photoelectron spectroscopy

1. Introduction

Copper (Cu) has been studied extensively as a potential substitute for aluminium (Al) and Al-alloys in multilevel-metallization of semiconductor devices and integrated circuits [1]. Compared with Al and Al-alloys, Cu has a number of beneficial factors, such as lower bulk resistivity, higher electromigration resistance, higher melting point, and lower reactivity with commonly used diffusion barrier materials. However, Cu has its drawbacks with respect to the applications in Si-based integrated circuits, such as difficulty in dry etching, poor adhesion to dielectric layers (SiO_2), fast diffusion in silicon and SiO_2, deep level trap in silicon, and formation of Cu silicides at low temperatures [1–3]. Meanwhile, another issue of interest concerns the easy oxidation of Cu exposed to the oxidizing ambient. It is well known that Cu oxidizes easily in air and in humid ambient [4], even at room temperature. This character has deferred the application of Cu in integrated circuits. Proper techniques must be developed to alleviate this problem before the application of Cu becomes feasible [5]. A number of studies have been reported that concern the oxidation-resistant Cu films doped with or covered by oxidation resistant metals [6–11]. Moreover, it has also been reported that the formation of metal silicide [12] on the surface of Cu films and the boron implantation into Cu films [13] provided superior oxidation resistance. In this study, thin films of the sputter deposited Cr—O and reactively sputter deposited Cr—N—O layers are used as resistant layers to protect Cu films from easy oxidation at high temperatures in an oxidizing ambient. In addition, we also evaluate the effects of thermal N_2 pre-sintering on the oxidation resistance of the Cr—O and Cr—N—O covered Cu films.

2. Experimental details

The starting materials were p-type boron-doped 3-inch diameter Si wafers with a nominal resistivity of 17–55 Ω cm. After an initial RCA cleaning [14], the Si wafers were thermally oxidized at 1050°C in steam atmosphere to grow 5000 Å of SiO_2. A 2000 Å Cu film was sputter deposited on the SiO_2 layer. This was followed by sputter deposition of a 200 Å thick cover-layer using a pure Cr target in an Ar ambient or in an ambient of (N_2+Ar) gas mixture at a pressure of 7.8 mTorr without breaking the vacuum. A DC magnetron sputtering system was used for the film deposition, and the base pressure of the system was about 1×10^{-6} Torr. Since Cr is an inherent oxygen absorber [15,16],

* Corresponding author. Tel.: + 886 3 5712121, ext. 54156; fax: +886 3 5724361; e-mail: mcchen@cc.nctu.edu.tw.

0040-6090/98/$ - see front matter
PII S0040-6090(98)00979-1

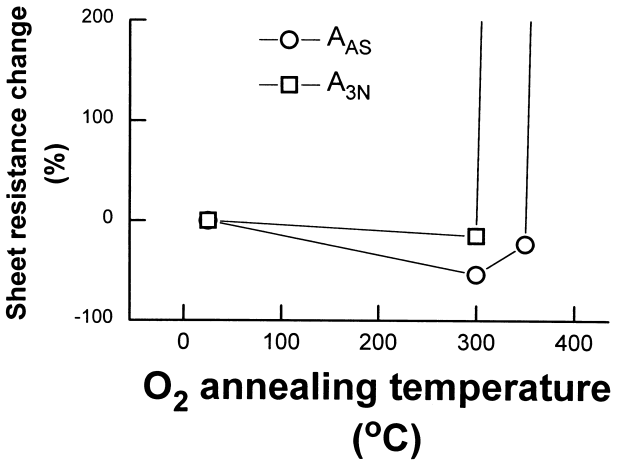

Fig. 1. Sheet resistance change vs. O_2 annealing temperature for samples A_{AS} and A_{3N}.

oxygen was automatically incorporated into the sputtered films. The layers sputter deposited in pure Ar ambient are designated as 'Cr—O' layers, while those reactively sputter deposited in (N_2+Ar) gas mixture with an N_2 partial pressure of 1.56 mTorr are designated as 'Cr—N—O' layers. The deposition rates of Cr—O and Cr—N—O layers were controlled to about 0.3 Å/s. The atomic concentration ratio of compositional elements in the Cr—N—O layer was Cr : N : O = 45 : 30 : 25, as determined by Auger electron spectroscopy (AES). For the simplicity of reference, the Cu films covered by Cr—O and Cr—N—O layers are designated as sample A and sample B, respectively. After the deposition of Cr—O or Cr—N—O layers, wafers were diced into 1.5×1.5 cm^2 pieces. The diced sample A's and sample B's were thermally sintered in an N_2 ambient for 30 min at 300, 500, and 700°C, and were further designated by subscripts of '3N', '5N', and '7N', respectively. Meanwhile, samples without N_2 sintering treatment were further designated by a subscript of 'AS' for identification. To study the resistance against Cu oxidation, each sample, with or without N_2 sintering treatment, was thermally annealed in an O_2 flowing furnace for 50 min at temperatures ranging from 100 to 600°C. For identification purpose, we designated, for example, sample A without N_2 pre-sintering treatment but thermally annealed at 500°C in O_2 as 'A_{AS}500O', and sample B with 500°C N_2 pre-sintering treatment and thermally annealed at 300°C in O_2 as 'B_{5N}300O'.

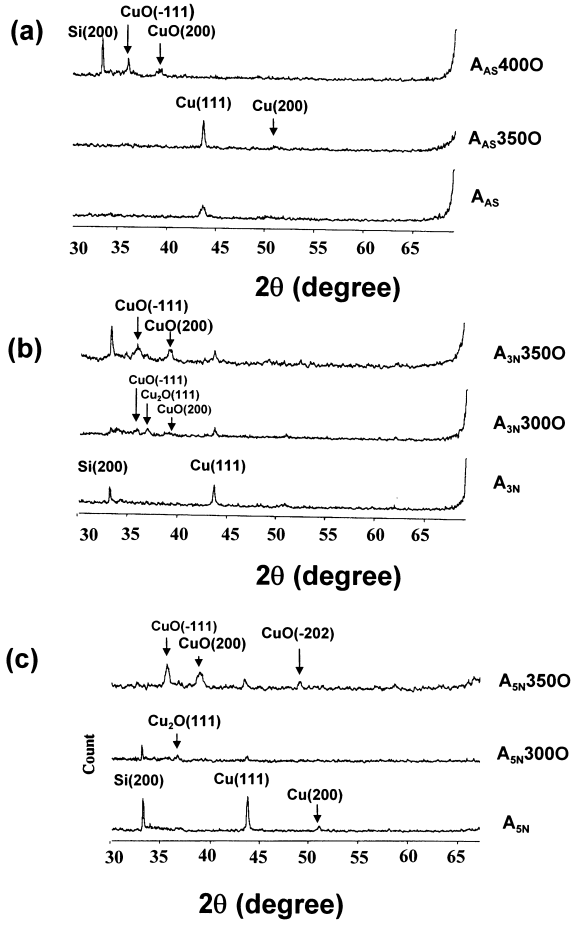

Fig. 2. XRD spectra for the O_2 annealed Cr—O/Cu/SiO_2/Si (sample A): (a) samples without N_2 pre-sintering treatment, (b) samples with N_2 pre-sintering treatment at 300°C and (c) samples with N_2 pre-sintering treatment at 500°C.

The abrupt sheet resistance change of samples was used as a criterion for failure of resisting Cu oxidation. The samples before and after the failure were further characterized by various techniques of material analysis. A 4-point probe was used to measure the sheet resistance. X-ray diffraction (XRD) analysis was used for phase identification. Scanning electron microscope (SEM) was used to investigate the surface morphology. Secondary ion mass spectroscopy (SIMS) was used for depth profile analysis. Moreover, X-ray photoelectron spectroscopy (XPS) was used to characterize the chemical states of compositional elements.

3. Results

3.1. Cr—O/Cu/SiO_2/Si

Fig. 1 shows the sheet resistance change for samples A_{AS} and A_{3N} after thermal annealing in O_2 ambient at a couple of temperatures. Abrupt change of sheet resistance was observed at temperatures higher than 350°C for sample A_{AS} and 300°C for sample A_{3N}. For samples A_{5N} and A_{7N}, which were N_2 pre-sintered at higher temperatures of 500 and 700°C, respectively, the abrupt change of sheet resistance occurred at an O_2 annealing temperature below 300°C; in addition, the oxidized films peeled off the SiO_2 substrate. Fig. 2 shows the XRD spectra for sample A's before and after annealing in O_2 ambient at temperatures around the abrupt change of sheet resistance. The spectra of sample A_{AS}'s, which were not N_2 pre-sintered, revealed (−111) and (200) orientations of CuO phase after O_2 annealing at 400°C (the A_{AS}400O spectrum); for the A_{AS} and the

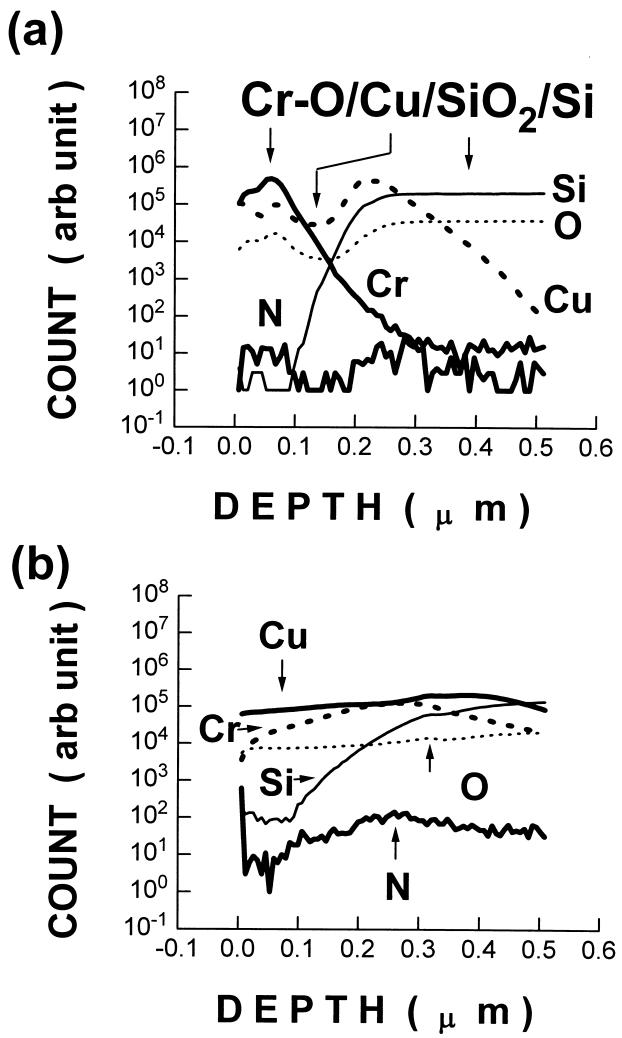

Fig. 3. SIMS depth profiles for the 300°C O_2 annealed samples A's: (a) sample without N_2 pre-sintering treatment (A_{AS}300O) and (b) sample with N_2 pre-sintering treatment at 500°C (A_{5N}300O).

A_{AS}350O samples, only Cu phase was observed; thus, the resistance against Cu oxidation of the Cr—O layer without N_2 pre-sintering treatment was defined to be 350°C. In contrast, copper oxide phases appeared on all the N_2 pre-sintered samples (samples A_{3N}, A_{5N}, and A_{7N}) after O_2 annealing at temperatures above 300°C (Fig. 2b,c) with the diminishing peak intensity of Cu(111) phase. Fig. 3 shows the SIMS depth profiles for samples A_{AS}300O and A_{5N}300O. It is clear that the sample A_{5N}300O had lost its original layered structure. This further confirms the degradation of the ability of resistance against Cu oxidation by N_2 pre-sintering treatment.

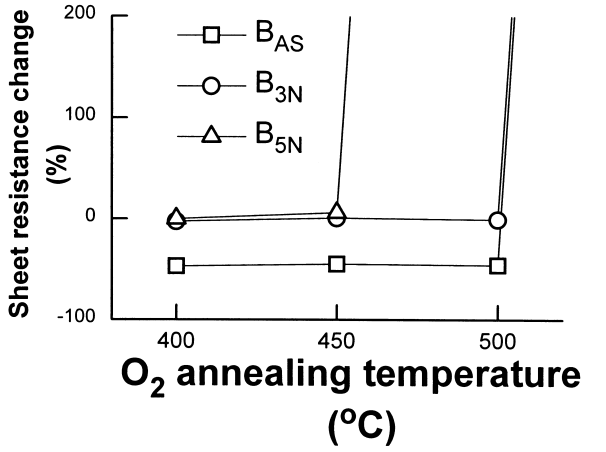

Fig. 4. Sheet resistance change vs. O_2 annealing temperature for samples B_{AS}, B_{3N} and B_{5N}.

3.2. Cr—N—O/Cu/SiO_2/Si

Fig. 4 shows the sheet resistance change for samples B_{AS}, B_{3N}, and B_{5N} after annealing in O_2 ambient at a number of temperatures. Abrupt change of sheet resistance was observed at temperatures higher than 500°C for sample B_{AS} as well as B_{3N} and 450°C for sample B_{5N}. By comparing the result for sample A_{AS} (Fig. 1) with that for sample B_{AS} (Fig. 4), we found that the ability of resistance against Cu oxidation of the Cr—N—O layer was 150°C higher than that of the Cr—O layer. However, similar to the case of Cr—O layer, N_2 pre-sintering treatment on the Cr—N—O layer degraded the ability of resistance against Cu oxidation too. Fig. 5 shows the XRD spectra for sample B's before and after annealing in O_2 ambient at temperatures around the occurrence of abrupt sheet resistance change. The spectra for samples B_{3N}'s (not shown) were similar to those of samples B_{AS}'s (Fig. 5a). The CuO phase appeared after 550°C annealing for sample B_{AS} while only Cu(111) phase was observed for the samples annealed at as well as below 500°C. However, for the 500°C N_2 pre-sintered samples (samples B_{5N}'s), the CuO phase appeared after O_2 annealing at 500°C (Fig. 5b). Fig. 6 shows the SIMS depth profiles for samples B_{AS}500O and B_{5N}500O. The loss of layered structure for sample B_{5N}500O (Fig. 6b) indicated the degradation of the ability of resistance against Cu oxidation by N_2 pre-sintering treatment.

Based on the illustration presented above, we concluded that the appearance of CuO phase coincided with the abrupt change of sheet resistance, which is an indication of the loss of layered structure of Cr—O/Cu/SiO_2/Si as well as Cr—N—O/Cu/SiO_2/Si.

4. Discussion

4.1. Implication of abrupt sheet resistance change

Decrease in sheet resistance was observed for the thermally O_2 annealed samples A_{AS} and A_{3N} with annealing temperature up to the occurrence of abrupt sheet resistance change, as shown in Fig. 1. In addition, XRD spectra showed increasing peak intensity of the Cu phase (Figs. 2a, and 5a,b) after annealing at temperatures just slightly below that for the appearance of Cu oxide phase for samples

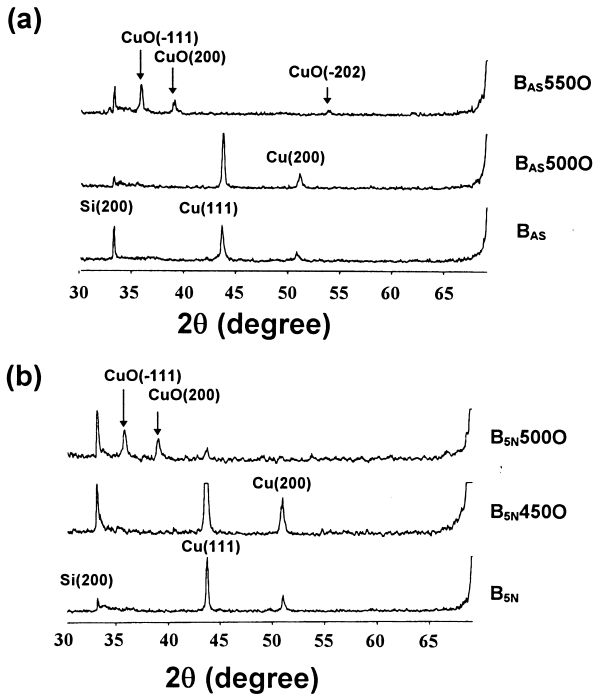

Fig. 5. XRD spectra for the O_2 annealed Cr—N—O/Cu/SiO_2/Si (sample B): (a) samples without N_2 pre-sintering treatment and (b) samples with N_2 pre-sintering treatment at 500°C.

A's as well as samples B's. The chemical states analyzed by XPS indicated that, before the abrupt sheet resistance change, the Cu photoelectrons remained in their elemental states and no Cu oxide states were detected; however, Cr oxide was detected on the outermost surface of the Cr—O/Cu/SiO_2/Si and Cr—N—O/Cu/SiO_2/Si structures. Thus, the thermal O_2 annealing at temperatures below the occurrence of abrupt sheet resistance change was merely a Cu film annealing process, which caused the oxidation of the Cr—O as well as the Cr—N—O layers.

For samples B_{7N}, which were N_2 pre-sintered at a high temperature of 700°C, abrupt change of sheet resistance occurred after O_2 annealing at temperatures as low as 400°C; moreover, the oxidized films were easily stripped off from the SiO_2 substrate, indicating complete oxidation of Cu layer due to the failure of Cr—N—O layer. Similar phenomenon, although to a less extent, was observed for samples A_{5N}'s, which were N_2 pre-sintered at 500°C. The stripping of the oxidized film was presumably due to the mismatch of expansion stress between the Cu oxide and the SiO_2 substrate in the absence of a glue layer of unreacted Cu.

4.2. Effect of reactively sputter introduced nitrogen

Figs. 7 and 8 show the surface morphology for the as-deposited and N_2 pre-sintered samples A's and samples B's, respectively. As shown in Fig. 7a, there were cracks and voids on the surface of sample A_{AS}. On the other hand,

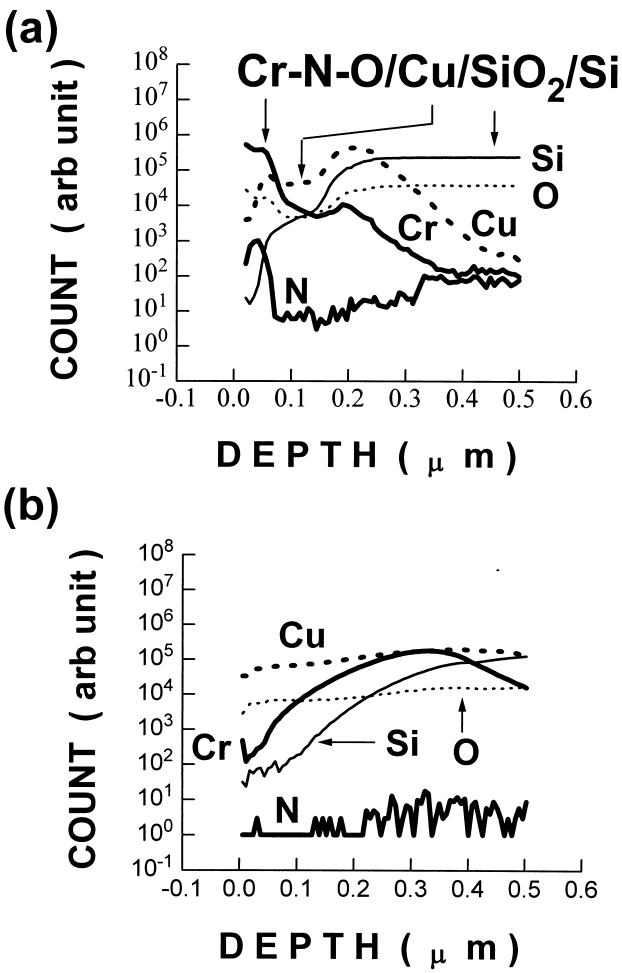

Fig. 6. SIMS depth profiles for the 500°C O_2 annealed samples B's: (a) sample without N_2 pre-sintering treatment (B_{AS}500O) and (b) sample with N_2 pre-sintering treatment at 500°C (B_{5N}500O).

sample B_{AS} revealed a shiny and smooth surface, as shown in Fig. 8a. The defects presented on the surfaces of the as-deposited Cr—O layers were presumably due to volume expansion of the Cr layer by oxygen absorption as well as the stress mismatch between the Cr—O and the Cu layers [16,17]. For the Cr—N—O layer of sample B, nitrogen was incorporated during the reactive sputter deposition [3,5]. Fig. 9 illustrates the XPS spectrum of N1s photoelectrons in the Cr—N—O layers. It showed that the N1s photoelectrons were present in elemental as well as nitride (Cr_2N) state [18]. The nitrogen tended to decorate the grain boundaries [3,15] as well as nitrify the Cr—N—O layer; this resulted in Cr—N—O layers of better compliance to accommodate the mismatch induced by the stress existing between Cu and Cr—N—O layers [1,3,16]. We expected that the nitrogen stuffed Cr nitride layer of sample B_{AS} should possess superior capability of resisting the diffusion of oxygen and of Cu, and thus possesses better resistance against Cu oxidation than the defected Cr—O layer of sample A_{AS} [3,6–13]. As we reported in Section 3, the ability of resistance against Cu oxidation of the as-deposited

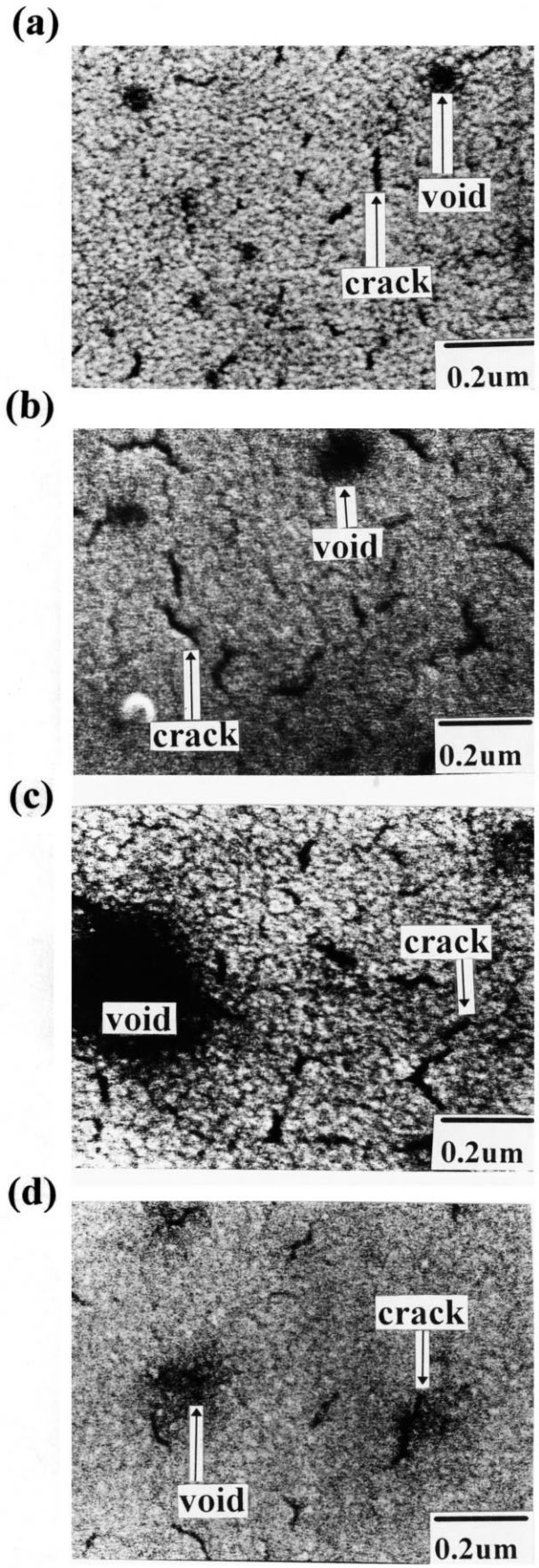

Fig. 7. SEM micrographs showing surface morphology of samples A's: (a) without N_2 pre-sintering treatment (A_{AS}), (b) with N_2 pre-sintering treatment at 300°C (A_{3N}), (c) with N_2 pre-sintering treatment at 500°C (A_{5N}) and (d) with N_2 pre-sintering treatment at 700°C (A_{7N}).

Cr—N—O layers was actually 150°C higher than that of the as-deposited Cr—O layers.

4.3. Effect of N_2 pre-sintering treatment

The comparison of SIMS depth profiles between samples A_{AS} and A_{5N} and that between samples B_{AS} and B_{5N} are illustrated in Figs. 10 and 11, respectively. For sample A, the N_2 pre-sintering treatment resulted in nitrogen incorporation into the Cr—O layer. However, the N_2 pre-sintering treatment did not heal the inherent defects in the Cr—O layer (Fig. 7b–d). Thus, the nitrogen incorporation in the Cr—O layer did not improve the resistance against Cu oxidation because of the unhealed defects, i.e. cracking of the films.

For sample B, however, the N_2 pre-sintering treatment did not result in obvious change of the nitrogen profile. The SIMS depth profiles of the compositional elements for the N_2 pre-sintered sample B_{5N} remained nearly the same as those of the as-deposited sample B_{AS}, except that the Cr profile showed a pile-up at the Cu/SiO_2 interface (Fig. 11). Pile-up of Cr at the Cu/SiO_2 interface was also observed for the N_2 pre-sintered sample A (Fig. 10). Moreover, the surface morphology of sample B_{3N} looked similar to that of sample B_{AS}, which was smooth and defect-free (Fig. 8a). Voids were found on the surface of samples B_{5N} and B_{7N} (Fig. 8b,c). The Cr pile-up at the Cu/SiO_2 interface indicated that Cr atoms diffused into/through Cu layer because the diffusivity of Cr in Cu film is higher than that of Cu in Cr film [15,16]. Presumably, the much more moved Cr led to coalescence of vacancies into void [17] on the surface of N_2 pre-sintered samples (Figs. 7 and 8). Besides, the agglomeration of thin films at elevated temperatures due to the mismatch of thermal expansion coefficient between Cr—N—O and Cu as well as the volume difference of Cr and Cr nitride might also contribute to the formation of voids. Moreover, grain growth of Cr—N—O layers due to the high temperature N_2 pre-sintering treatment resulted in shorter diffusion paths for the oxidation species (i.e. Cu and oxygen), especially for the thin layers used in this study. Thus, Cu and oxygen diffused through these paths more easily, resulting in the degradation of the resistance against Cu oxidation for the N_2 pre-sintered samples.

From the data presented above, it is clear that N_2 pre-sintering treatment caused degradation of the resistance against Cu oxidation for both Cr—O and Cr—N—O layers, though the pre-sintering temperature that would induce degradation was different for the Cr—O and Cr—N—O layers. It was 300°C for the former layer and was 500°C for the latter layer. As stated above, the inherent defect in samples A's was regarded as the major cause of this differ-

ence. The nitrogen stuffed Cr-nitride layers (sample B) were more compliant than the nitrogen deficient Cr—O layers (sample A). A much higher pre-sintering temperature was required for the Cr—N—O layers to form void and grow their grains.

5. Summary and conclusion

This work studied the resistance against Cu oxidation of sputter deposited Cr—O and reactively sputter deposited Cr—N—O layers of 200 Å thickness with and without ther-

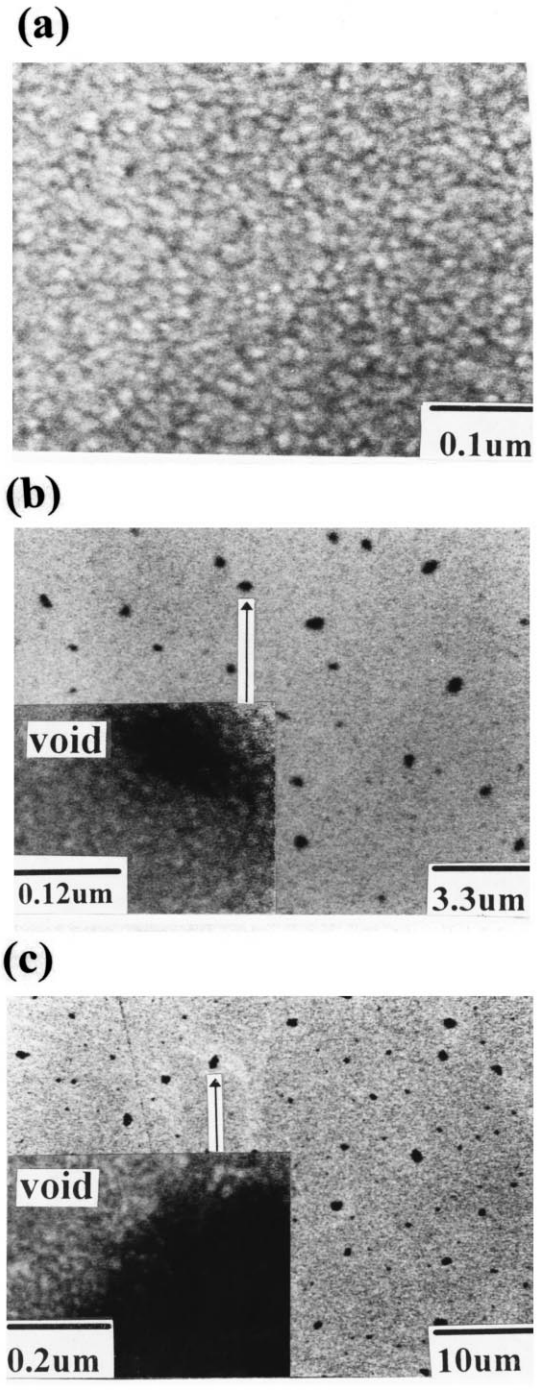

Fig. 8. SEM micrographs showing surface morphology of samples B's: (a) without N_2 pre-sintering treatment (B_{AS}), (b) with N_2 pre-sintering treatment at 500°C (B_{5N}) and (c) with N_2 pre-sintering treatment at 700°C (B_{7N}).

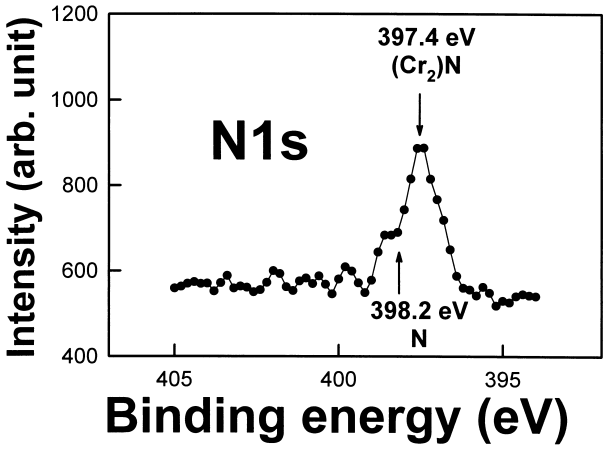

Fig. 9. XPS spectrum showing the chemical states of N1s photoelectrons for the nitrogen incorporated in the Cr—N—O layer.

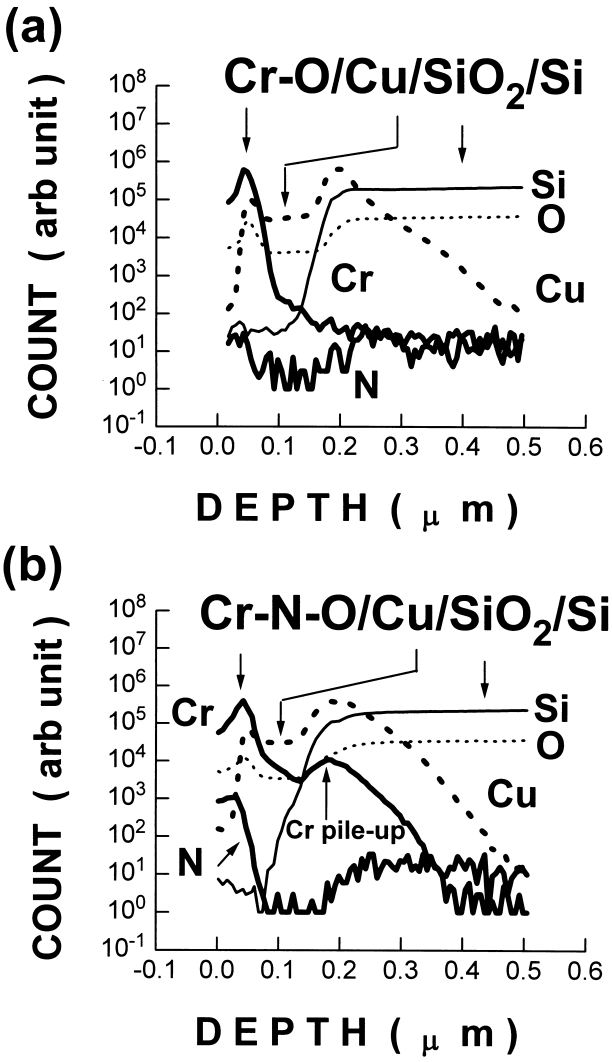

Fig. 10. SIMS depth profiles for samples A's: (a) without N_2 pre-sintering treatment (A_{AS}) and (b) with N_2 pre-sintering treatment at 500°C (A_{5N}).

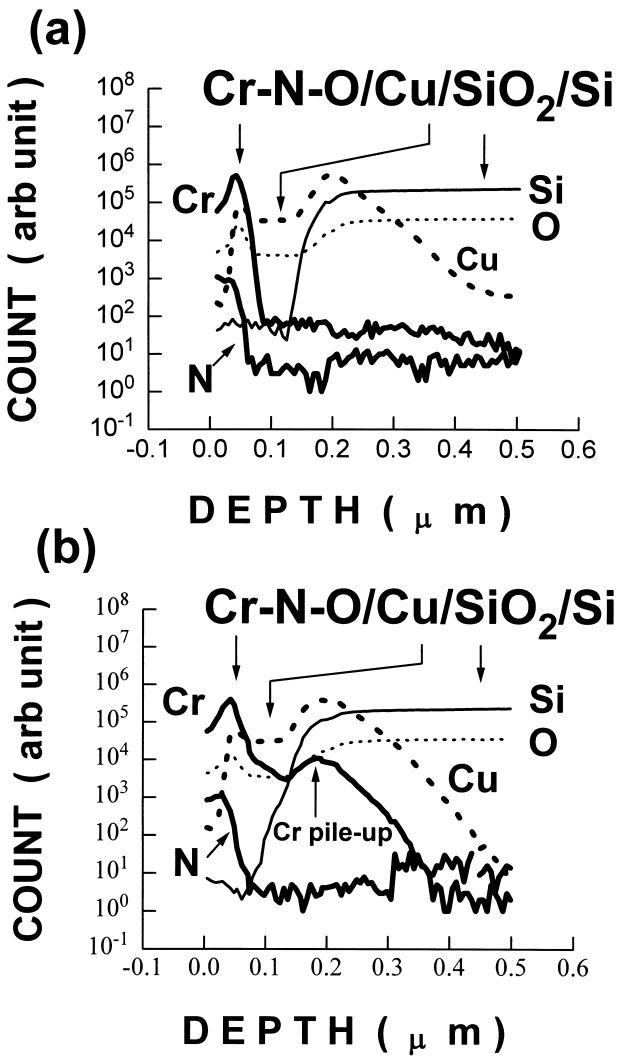

Fig. 11. SIMS depth profiles for samples B's: (a) without N_2 pre-sintering treatment (B_{AS}) and (b) with N_2 pre-sintering treatment at 500°C (B_{5N}).

mal N_2 pre-sintering treatment. The Cr—O covered Cu films can resist thermal annealing in O_2 ambient at temperatures up to 350°C, while the Cr—N—O covered Cu films can resist the same treatment at temperatures up to 500°C, all without causing Cu oxidation. The distinction of the resistance against Cu oxidation was presumably due to the inherent defects, including cracks and voids, in the Cr—O film, and the nitrogen doping in the Cr—N—O film. With N_2 pre-sintering treatment on the Cr—O or Cr—N—O covered Cu films, the resistance against Cu oxidation was degraded. The higher the N_2 pre-sintering temperature was, the lower the oxidation temperature of Cu became. The unhealed defects of N_2 pre-sintered Cr—O layers were presumed to be the principal reason of degradation for the Cr—O case. On the other hand, voids formation after N_2 pre-sintering treatment at elevated temperatures was regarded as the cause of degradation for the Cr—N—O case. Nitrogen in the Cr—N—O layers decorated the grain boundaries of Cr nitride and improved the surface morphology of the layers, resulting in a better resistance against Cu oxidation than that of the Cr—O layer. Since the beneficial effect of nitrogen doping may be outweighed by the formation of voids during the N_2 pre-sintering process, we conclude that the N_2 pre-sintering treatment is an excess thermal treatment, and should be avoided in the application of Cr—O or Cr—N—O film as resistant layer against Cu oxidation.

Acknowledgements

The authors wish to thank the Semiconductor Research Center of National Chiao-Tung University for providing excellent processing environment. This work was supported by the National Science Council, ROC, under contract no. NSC-86-2215-E-009-040.

References

[1] Copper-based Metallization and Interconnects for Ultra-Large-Scale Integration Applications (special issue), Thin Solid Films 262 (1995).
[2] J.D. McBrayer, R.M. Swanson, T.W. Sigmon, J. Electrochem. Soc. 133 (1986) 1242.
[3] S.Q. Wang, S. Suthar, C. Hoeflich, B.J. Burrow, J. Appl. Phys. 73 (1993) 2301.
[4] J. Li, J.W. Mayer, E.G. Colgan, J. Appl. Phys. 70 (1991) 2820.
[5] C.-K. Hu, B. Luther, F.B. Kaufman, J. Hummel, C. Uzoh, D.J. Pearson, Thin Solid Films 262 (1995) 84.
[6] W.A. Lanford, P.J. Ding, W. Wang, S. Hymes, S.P. Murarka, Thin Solid Films 262 (1995) 234.
[7] P.J. Ding, W. Wang, W.A. Lanford, S. Hymes, S.P. Murarka, Appl. Phys. Lett. 65 (1994) 1778.
[8] J. Li, J.W. Mayer, Y. Shacham-Diamand, E.G. Colgan, Appl. Phys. Lett. 60 (1992) 2983.
[9] H. Itow, Y. Nakasaki, G. Minamihaba, K. Suguro, H. Okano, Appl. Phys. Lett. 63 (1993) 934.
[10] D.S. Gardner, J. Onuki, K. Kudoo, Y. Misawa, Q.T. Vu, Thin Solid Films 262 (1995) 104.
[11] Y. Igarashi, T. Yamanobe, T. Yamaji, S. Nishikawa, T. Ito, Jpn. J. Appl. Phys. 33 (1) (1994) 462.
[12] S. Hymes, S. P. Murarka, C. Shepard, W.A. Lanford, J. Appl. Phys. 71 (1992) 4623.
[13] P.J. Ding, W.A. Lanford, S. Hymes, S.P. Murarka, J. Appl. Phys. 74 (1993) 1331.
[14] W. Kern, D.A. Puotinen, RCA Rev. 31 (1970) 187.
[15] E.A. Brandes, Smithells Metals Reference Book, 6th ed., Robert Hartnoll, Bodmin, 1983, pp. (8–21)– (8–25).
[16] D.R. Lide (Ed.), CRC Handbook of Chemistry and Physics, 73rd ed., CRC Press, Boca Raton, Florida, 1992, Section 12: Properties of Solids.
[17] R.E. Reed-Hill, Physical Metallurgy Principles, 2nd ed., Van Nostrand, New York, 1972, pp. 386–390.
[18] G.E. Muilenberg (Eds.), Handbook of X-ray Photoelectron Spectroscopy, Perkin-Elmer Corporation, Physical Electronics Division, Eden Prairie, Minnesota, 1979.